Reorientation effect and electrical current in a weakly anchored nematic cell

R. Teixeira de Souza, M. M. A. de Jesus, J. C. Dias, and L. R. Evangelista
Departamento de Física, Universidade Estadual de Maringá Avenida Colombo, 5790-87020-900 Maringá, Paraná, Brazil
(Received 31 March 2009; revised manuscript received 6 July 2009; published 7 October 2009)

A nematic cell subjected to a large electric field undergoes a molecular reorientation that affects the electrical current flowing through it. To analytically establish the dependence of the current on the applied voltage, the cell is considered as parallel of resistance, $R(t)$, and capacitance, $C(t)$, that are connected with the nematic director profile. This profile is determined in the quasistatic regime in which the nematic orientation follows the time variation in the external field normal to the cell plates without delay. The analysis performed for a weakly anchored cell shows that the current presents a peak when the applied voltage overcomes the threshold voltage for the transition of Fréedericksz at a critical time t^* as in the case of strong anchoring. For large voltages, $R(t)\rightarrow R_{\parallel}$ and $C(t)\rightarrow C_{\parallel}$, where $\parallel$ refers to the nematic director. We show that, for large enough time $t \gg t^*$, it is possible to connect the measured current with the extrapolation length characterizing the sample by means of simple analytical expressions. This connection can be used to experimentally estimate the anchoring energy by means of current measurements.

DOI: 10.1103/PhysRevE.80.041702 PACS number(s): 83.80.Xz, 66.10.−x, 82.45.Gj, 72.80.−r

I. INTRODUCTION

When an electric field applied to a uniformly oriented nematic liquid-crystal (NLC) sample overcomes the threshold field for Fréedericksz transition, reorientational effects strongly affect the electrical response of the cell [1–3]. In particular, the time response of the director to a stepwise electric field, which evidences the characteristic slow dynamics in weak anchoring situation [4], has to be taken explicitly into account to correctly investigate the orientation response of a weakly oriented nematic cell. If the liquid-crystalline cell can be considered as parallel of resistance, R, and capacitance, C, these quantities will vary as the deformation is induced by the external voltage [5–8]. In fact, the measured current flowing through the circuit may present a peak in correspondence to the threshold voltage as recently shown in strong anchoring situation [9]. If the anchoring is weak, it is expected that as the applied voltage increases with time the values of the resistance and the capacitance increase toward the values $R_{\parallel}$ and $C_{\parallel}$, where $\parallel$ refers to the nematic director **n** that represent the values of a uniformly oriented homeotropic sample because the molecules follow the orienting effect of the field in the entire sample [10]. This means that, for large enough applied voltage, it is possible to replace the original nematic cell by an equivalent cell with two identical halves having a hybrid orientation. This permits to obtain simple analytical expressions for $R(t)$ and $C(t)$ and consequently for the total current $I(t)$, which represent very well the exact quantities of the original cell. In this manner, the expression for the current can be written as a function of the extrapolation length and, in principle, could be used to estimate the anchoring energy of the cell directly from the current measurements.

This paper is organized as follows. In Sec. II, we present the formalism connecting R and C with the profile of the director in an NLC cell in the situation of weak anchoring for a sample in the shape of a slab limited by two identical surfaces. In Sec. III, the equations for the electrical problem are established and the temporal behavior of R, C, and I are numerically investigated. In Sec. IV, the role of the anchoring energy is analytically investigated by means of the "hybrid cell" approximation. Some concluding remarks are drawn in Sec. V.

II. TILT ANGLE PROFILE OF AN NLC CELL IN WEAK ANCHORING

Let us consider a nematic sample limited by two parallel plates normal to the z axis, placed at $z=\pm d/2$. This sample having a surface area A is connected to the external power supply whose time-dependent electromotive force is $V(t)$ with a period $4T$. In this case, the nematic director will follow the time variation of the applied voltage. Consequently, the director field depends on z and t and, if only splay-bend deformations are allowed, it has components in the x and z directions. If $\theta(z,t)$ is the angle formed by **n** with the x axis, in the one constant approximation ($K_{11}=K_{33}=K$), the dynamical equation for $\theta(z,t)$ has the form

$$K\frac{\partial^2\theta(z,t)}{\partial z^2}+\frac{\epsilon_a V^2(t)}{2d^2}\sin 2\theta(z,t)=\eta\frac{\partial\theta}{\partial t}, \tag{1}$$

where η is the coefficient of rotational viscosity of the nematic liquid crystal [11], and $\epsilon_a=\epsilon_{\parallel}-\epsilon_{\perp}$ is the dielectric anisotropy, where $\parallel$ and $\perp$ refer to the director orientation. In what follows, ϵ_a will be assumed as positive and the initial orientation is the uniform planar one. If T is greater than the characteristic time for the reorientation of the cell, $\tau=\eta d^2/(\pi^2 K)$, the director will follow the field without delay. Using physical parameters typical of a liquid-crystalline material one obtains $\tau\approx 0.03$ s, such that $\tau \ll T$ (which is in the order of seconds) [9].

In this situation, the quasistatic regime is a good approximation and the director profile may be obtained by solving the equation:

$$\frac{\partial^2\theta(z,t)}{\partial z^2} + \frac{\epsilon_a V^2(t)}{2Kd^2}\sin 2\theta(z,t) \approx 0, \tag{2}$$

with the appropriate boundary conditions for weak anchoring. To establish them, we assume identical surfaces in the Rapini-Papoular [12] approximation for the surface energy given by

$$f_{\text{surf}} = \frac{1}{2}W\sin^2(\theta_S - \Theta), \tag{3}$$

in which W is the anchoring strength, Θ is the tilt angle imposed by the surface, and $\theta_S(t)=\theta(\pm d/2,t)$ is the tilt angle at the surfaces. In this framework, for uniform planar anchoring ($\Theta=0$), the boundary condition to be satisfied by the solution of Eq. (2) is

$$\pm \left.\frac{\partial\theta(z,t)}{\partial z}\right|_{z=\pm d/2} + \frac{1}{2L}\sin 2\theta\left(\pm\frac{d}{2},t\right) = 0, \tag{4}$$

where $L=K/W$ is the extrapolation length. $\theta(z,t)$ has a maximum at $z=0$ denoted by $\theta(z=0,t)=\theta_{\text{M}}(t)$. The solution for Eq. (2) together with Eq. (4) can be put in the form

$$\int_{\theta_S(t)}^{\theta(z,t)} \frac{d\theta}{\sqrt{\sin^2\theta_{\text{M}}(t) - \sin^2\theta}} = \frac{1}{\xi(t)}\left(\mp z + \frac{d}{2}\right), \tag{5}$$

where "−" refers to the interval $-d/2<z<0$ and "+" to $0<z<d/2$ and

$$\sin\theta_{\text{M}}(t) = \sin\theta_{\text{S}}(t)\sqrt{\left(\frac{\xi(t)}{L}\right)^2\cos^2\theta_{\text{S}}(t) + 1}, \tag{6}$$

where

$$\xi(t)^{-1} = \frac{\pi}{d}\frac{V(t)}{V_{\text{th}}}$$

is the coherence length [2] and $V_{\text{th}}=\pi\sqrt{K/\epsilon_a}$ is the threshold voltage for the strong anchoring situation [13]. For computational purposes, we define $\sin\psi=\sin\theta/\sin\theta_{\text{M}}$, and for $z=0$, we obtain from Eq. (5) a relation connecting $\theta_M(t)$ with $\theta_{\text{S}}(t)$ in the form

$$\int_{\psi_S(t)}^{\pi/2} \frac{d\psi}{\sqrt{1-\sin^2\theta_{\text{M}}(t)\sin^2\psi}} = \frac{d}{2\xi(t)}, \tag{7}$$

where $\psi_{\text{S}}(t)=\arcsin[\sin\theta_{\text{S}}(t)/\sin\theta_{\text{M}}(t)]$. Equations (6) and (7) can be solved for any t to determine $\theta_M(t)$ and $\theta_{\text{S}}(t)$, which, in turn, can be used in Eq. (5) to establish the tilt-angle profile $\theta(z,t)$.

For our analysis, the time dependence of the voltage shown in Fig. 1 has the form

$$V(t) = \kappa t\{(\vartheta[t] - \vartheta[t-T]) + (2T-t)(\vartheta[t-T] - \vartheta[t-3T]) + (t-4T)\vartheta[t-3T]\}, \tag{8}$$

where $\vartheta[x]$ is the step function: $\vartheta[x]=0$ for $x<0$, and $\vartheta[x]=1$ for $x>0$, $\kappa=V_0/T$, and $V(t=T)=V_0$ is the amplitude of the applied potential. We limit our analysis to the positive cycle from $t=0$ at $t=2T$. The behavior of the director in the middle of the sample, $\theta_M(t)$, is affected by the electric force on the molecules. If the elastic forces are stronger than this force, the director remains uniformly oriented. But since the voltage increases with time, a value of the electric force exists such that the uniform orientation becomes unstable, and the director field is deformed. This is the Fréedericksz transition, for which a threshold voltage can obtained from Eq. (7) in the limit $\theta_{\text{M}}\to 0$. In weak anchoring situation we are considering here, the critical voltage V_{th}^* is given by

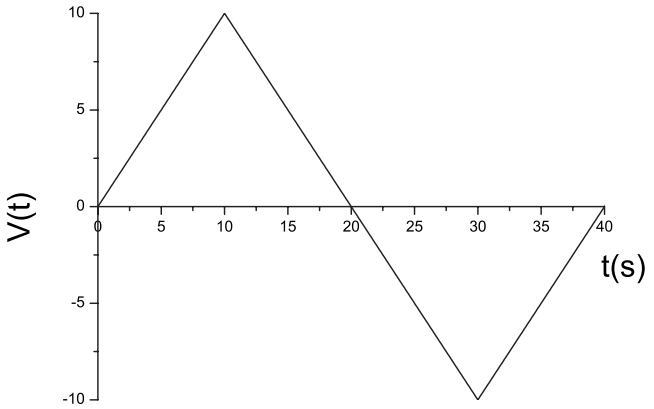

FIG. 1. Time dependent electric potential as given by Eq. (8) for $V_0=10$ V and $T=10$ s.

$$\cot\left[\frac{\pi}{2}\frac{V_{\text{th}}^*}{V_{\text{th}}}\right] = \frac{\pi L}{d}\frac{V_{\text{th}}^*}{V_{\text{th}}}. \tag{9}$$

In Fig. 2, the roots of Eq. (9) are shown as a function of the ratio $2L/d$. One easily deduces that

$$\frac{V_{\text{th}}^*}{V_{\text{th}}} \to 1 \quad \text{as} \quad \frac{L}{d} \to 0$$

and

$$\frac{V_{\text{th}}^*}{V_{\text{th}}} \to 0 \quad \text{as} \quad \frac{L}{d} \to \infty.$$

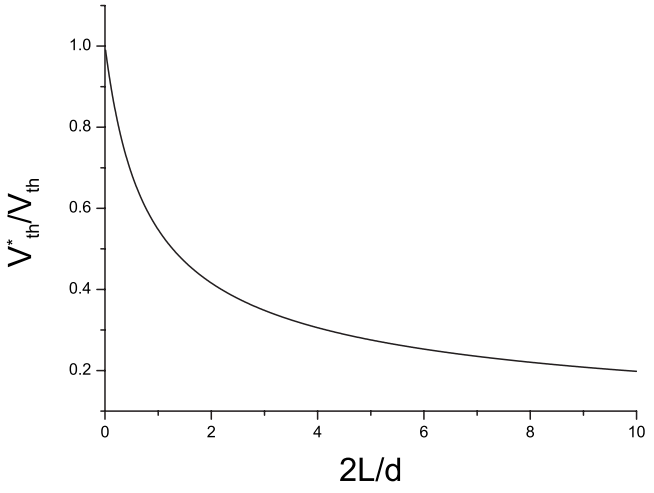

FIG. 2. Behavior of $V_{\text{th}}^*/V_{\text{th}}$ for different values of ratio $2L/d$ as predicted by Eq. (9). As expected, in the limit of strong anchoring, $V_{\text{th}}^*\to V_{\text{th}}$; in the extremely weak anchoring limit $V_{\text{th}}^*\to 0$.

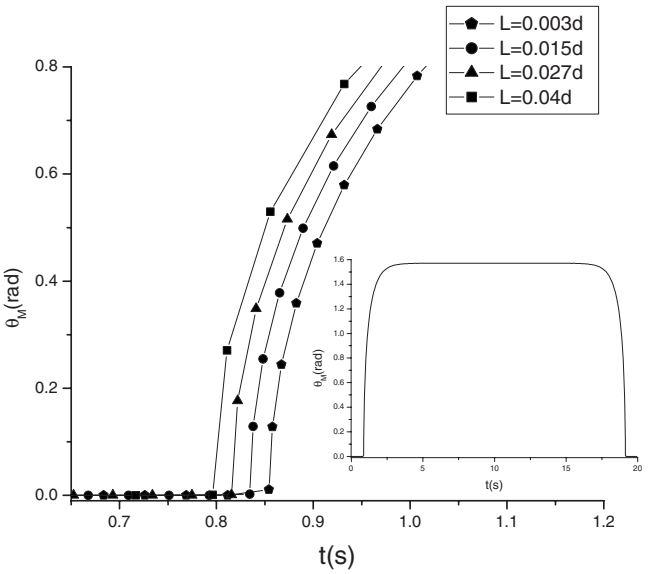

FIG. 3. Behavior of θ_M with t near $t=t^*$ for different values of the extrapolation length L. The inset exhibits the interval $0 \leq t \leq 2T$.

We denote by t^* the critical time for which $V(t^*)=V_{th}^*$. Therefore, the dependence of θ_S and θ_M on t is not smooth. In fact, both $\theta_S(t)$ and $\theta_M(t)$ would have vertical tangents at $t=t^*$, and the first derivatives would be infinite. For the numerical analysis we use the physical parameters $V_0=10$ V, $\varepsilon_{\parallel}=20.6\varepsilon_0$, $\varepsilon_{\perp}=5.5\varepsilon_0$, $\sigma_{\parallel}=10^{-10}$ $(\Omega m)^{-1}$, $\sigma_{\perp}=5\sigma_{\parallel}$, $K=10^{-11}$ N, $d=5\times10^{-6}$ m, and $A=10^{-4}$ m^2. The behavior of $\theta_M(t)$ is shown in Fig. 3 for a small interval near $t=t^*$ and for the entire cycle $(0 \leq t \leq 2T)$ (inset) for representative values of the extrapolation length L. The behavior of $\theta_S(t)$ is shown in Fig. 4 for the same set of parameters.

III. ELECTRIC CELL-FUNDAMENTAL EQUATIONS

To focus on the influence of the reorientation phenomenon on the electrical response of the sample, the role of the Debye layer [7,14] connected with the presence of ions responsible for the electrical conduction in liquid crystals will be neglected. In our analysis, we assume that the electrodes are perfectly conducting in such a manner that there is no confinement of the ions in the surface layers. In this case, the net bulk density of charge is zero. In the opposite case, where the electrodes are blocking, the ions are confined in a surface layer whose thickness is of the order of the Debye screening length. In this situation, the actual electric field in the sample is position dependent and has to be determined by solving the equation of Poisson. The analysis for this case is under study and will be published elsewhere. On the other hand, even if the sample may be considered as free of ions, both the conductivity and the dielectric susceptibility are inhomogeneous and anisotropic. This would imply that the electric field inside the sample should be nonuniform, and in the geometry we are considering it would be z dependent. In this manner, a coupling of the electric field and the nematic director could have a noticeable effect on the actual values of the tilt-angle field [15]. However, this effect is small on the saturation behavior of $\theta_M(t)$ and can be neglected here because the hybrid cell approximation used in Sec. IV works very well when $\theta_M(t) \approx \pi/2$, i.e., for $V > V_{th}$. Consequently, the electric field across the sample will be considered uniform and coinciding with the external one. In this situation, when an NLC is under the action of an external voltage, the sample can be faced as a parallel between a resistance and a capacitance. For an NLC sample in a uniform planar orientation, these quantities are simply $R_{\perp}$ and $C_{\perp}$. However, since the applied voltage is time dependent, the orientation of the molecules will change and R and C will become time-dependent functions. This time dependence comes from the tilt-angle distribution in the form

$$R(t) = \frac{1}{A}\int_{-d/2}^{d/2} \frac{dz}{\sigma_{\perp} + \sigma_a \sin^2 \theta(z,t)} \quad \text{and}$$

$$\frac{1}{C(t)} = \frac{1}{A}\int_{-d/2}^{d/2} \frac{dz}{\epsilon_{\perp} + \epsilon_a \sin^2 \theta(z,t)}, \tag{10}$$

where $\sigma_a=\sigma_{\parallel}-\sigma_{\perp}$ is the anisotropy in the conductivity. For $t<t^*$, the sample is in a planar orientation and $\theta(z,t)=0$; in this case, both the resistance and the capacitance have the usual form characteristic of isotropic materials, i.e.,

$$R(t) = R_{\perp} = \frac{d}{\sigma_{\perp} A} \quad \text{and} \quad C(t) = C_{\perp} = \epsilon_{\perp}\frac{A}{d}.$$

Likewise, it is expected [10] that for $t \gg t^*$, when $\theta(z,t) \to \pi/2$,

$$R(t) = R_{\parallel} = \frac{d}{\sigma_{\parallel} A} \quad \text{and} \quad C(t) = C_{\parallel} = \epsilon_{\parallel}\frac{A}{d}.$$

In fact, these limiting values are easily found in Fig. 5, where the behavior of the $R(t)$ [Fig. 5(a)] and $C(t)$ [Fig. 5(b)] is shown for some values of the ratio L/d. Notice that even if $C(t)$ and $R(t)$ are continuous quantity at $t=t^*$ the same is not true for their derivatives which present a jump at the transition time. Figure 5(b) resembles the cell capacitance behav-

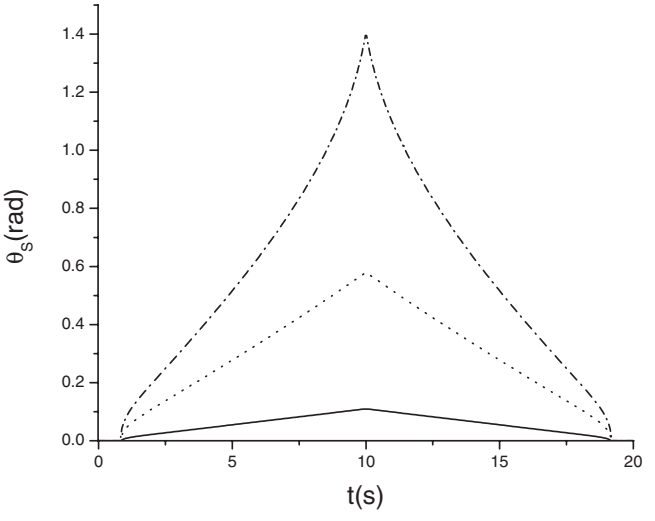

FIG. 4. Behavior of θ_S with t for the interval $0 \leq t \leq 2T$ for different values of the ratio $L/d=0.003$ (solid), 0.015 (dot), and 0.025 (dash dot).

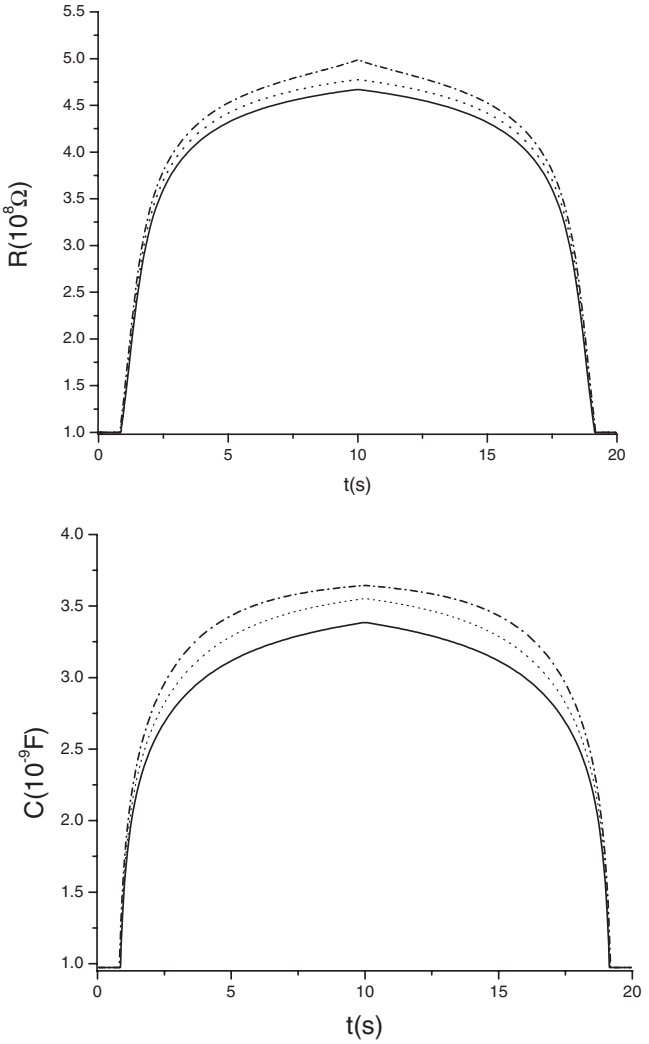

FIG. 5. $R(t)$ vs t and $C(t)$ vs t for the illustrative values of the ratio L/d shown in Fig. 4.

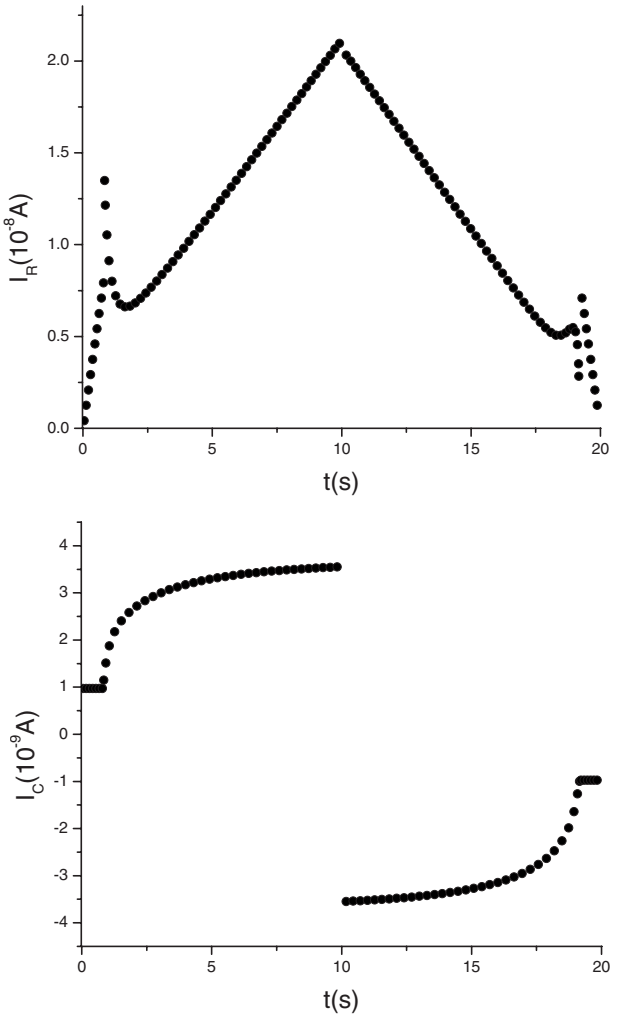

FIG. 6. Temporal behavior of the current in (a) the resistive part of the equivalent circuit and (b) in the capacitive part for $L=0.015d$.

ior close to the *N-I* transition point as a function of the applied bias as shown in Ref. [16].

The total electric current flowing through the cell is given by

$$I(t) = \frac{V(t)}{R_{\text{eff}}(t)} + C(t)\frac{dV(t)}{dt}, \tag{11}$$

where

$$\frac{1}{R_{\text{eff}}(t)} = \frac{1}{R(t)} + \frac{dC(t)}{dt}$$

is the effective resistance in the sample. Therefore, we can separate the part of the current flowing through the resistance from the one flowing through the capacitor in the form represent by $I(t)=I_R(t)+I_C(t)$. In Figs. 6(a) and 6(b), $I_R(t)$ and $I_C(t)$ are, respectively, shown as a function of t. In Fig. 7, the temporal behavior of the total current is shown and exhibits a discontinuity in correspondence with the discontinuity in the derivative of the capacitance. The most common situation corresponds to $\sigma_a>0$, differently from the illustrative case we are considering here. In fact, the peak in the current is easier found when $\sigma_a<0$. Furthermore, as we shall show below, for what concerns the analysis of the anchoring energy, the sign of σ_a does not change our results. Before proceeding, a remark about the numerical calculations is in order. They have been performed with the software MATHEMATICA. First, by using FINDROOT we have obtained $\theta_M(t)$ and $\theta_S(t)$ with an average accuracy of 10^{-6}. After that, we have obtained a first integral of Eq. (2) and, then, numerically solved the resulting first order differential equation. In this manner, the profile of the tilt angle $\theta(z,t)$ was obtained, and from these results, the capacitance and the resistance have been determined by numerical integration. Finally, by interpolation of the numerical data, with a very large number of points, we have obtained dC/dt with a good accuracy. All the calculations can be performed in a few minutes with a common PC.

IV. ROLE OF THE ANCHORING ENERGY

To explore the experimental connection between the measured current and the anchoring energy, we notice that when

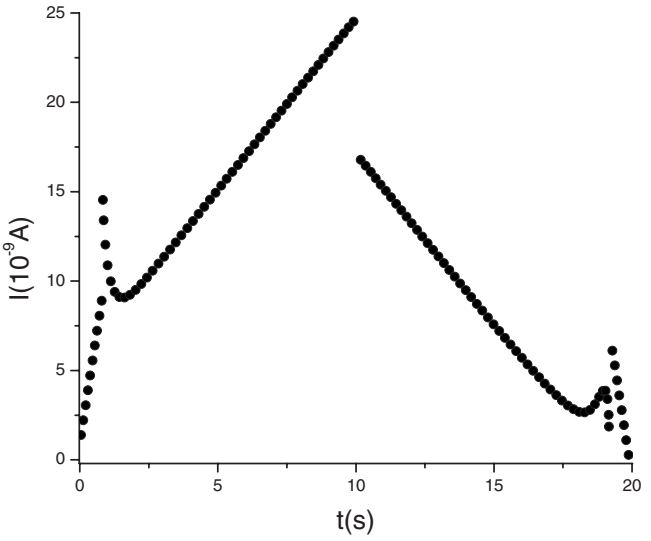

FIG. 7. Temporal behavior of the total current in the circuit in the cycle $0 \leq t \leq 2T$, $L=0.015d$.

$t \to T$ the applied voltage is much greater than the threshold voltage, and the center of the sample is essentially in a homeotropic alignment. Since the surfaces are identical, the situation for lower half of the cell is equivalent to a hybrid cell with one surface placed at $z=-d/2$, presenting a "pretilt" angle $\theta_S(t)$, and another surface located at $z=0$, in strong anchoring and such that $\theta(0,t)=\theta_M(t) \approx \pi/2$. The same "analogy" is valid for the upper half of the cell $(0 \leq z \leq d/2)$ as shown in Fig. 8. This analogy permits to establish an analytical connection between the measured current $I(t)$ and the anchoring energy W, as we shall shown below.

For the hybrid cell described before, the tilt angle is approximately given by [2]

$$\theta(z,t) = \frac{\pi}{2} - 2 \arctan[s(t)e^{-(z+d/2)/\xi(t)}], \tag{12}$$

where

$$s(t) = \tan\left[\frac{\pi}{4} - \frac{\theta_S(t)}{2}\right].$$

The solution $\theta(z,t)$ is such that $\theta(-d/2,t)=\theta_S(t)$ and

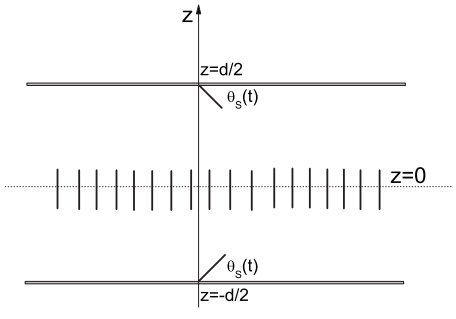

FIG. 8. Equivalent hybrid nematic cells. In the limit $\theta_M(t) \to \pi/2$ the center of the sample is in a "strong" homeotropic orientation, while the surface can be considered as having a pretilt $\theta_S(t)$.

$$\theta(0,t) \approx \frac{\pi}{2} - 2s(t)e^{-d/2\xi(t)} \approx \frac{\pi}{2} \tag{13}$$

because for $t \to T$, $V(T) \gg V_{th}$ and, consequently, $d \gg \xi(T)$. In this manner, the boundary condition at $z=0$ is satisfied in the limit we are considering. The solution involves now a pretilt angle which is truly the surface tilt angle given by Eq. (6) which, for $\theta_M=\pi/2$, is reduced to

$$\sin \theta_S(t) = \frac{L}{\xi(t)}. \tag{14}$$

By using Eq. (12) into Eqs. (10), we can perform the integrations to obtain

$$R(t) = R_{\parallel} - \frac{2\xi(t)}{A\sigma_{\parallel}}\sqrt{\frac{\sigma_a}{\sigma_{\perp}}}[\arctan X - \arctan Y] \tag{15}$$

for the resistance and

$$\frac{1}{C(t)} = \frac{1}{C_{\parallel}} - \frac{2\xi(t)}{A\epsilon_{\parallel}}\sqrt{\frac{\epsilon_a}{\epsilon_{\perp}}}[\arctan X - \arctan Y] \tag{16}$$

for the capacitance. In the above expressions, we have introduced the quantities

$$X = \frac{x_{\parallel} + (x_{\perp} - x_a)s(t)^2}{2\sqrt{x_a x_{\perp}}s(t)^2} \quad \text{and}$$

$$Y = \frac{x_{\parallel}e^{d/\xi(t)} + (x_{\perp} - x_a)s(t)^2}{2\sqrt{x_a x_{\perp}}s(t)^2}, \tag{17}$$

where $x_a=x_{\parallel}-x_{\perp}$ with $(x_{\parallel},x_{\perp})=(\sigma_{\parallel},\sigma_{\perp})$ for the resistance and $(x_{\parallel},x_{\perp})=(\epsilon_{\parallel},\epsilon_{\perp})$ for the capacitance. In Fig. 9, the temporal behavior of R and C, as predicted, respectively, by Eqs. (15) and (16), is shown in comparison with the exact values. The agreement for the resistance and for the capacitance is excellent for a large time interval. This means that for the time interval around $t=T$, Eqs. (15) and (16) are very good expressions for resistance and the capacitance of the cell. The total current in this time interval can be analytically determined and, in particular, at $t=T$ it becomes

$$I(T) = \frac{V_0}{R(T)} + V_0\left[\frac{dC(t)}{dt}\right]_{t=T} + C(T)\frac{V_0}{T}, \tag{18}$$

where we have used $V(T)=V_0$ and $(dV/dt)_{t=T^-}=V_0/T$. Notice that $(dV/dt)_{t=T^+}=-V_0/T$, but in the present analysis it is enough to consider what happens in the interval $0<t<T$. In Fig. 10 the total current calculated using Eqs. (15) and (16) into Eq. (11) is shown for the cycle $0 \leq t \leq 2T$. The agreement between the exact result and the approximated one is excellent for a very large time interval. This means that for the time interval $t \gg t^*$ all the $I(V)$ characteristics of the nematic cell in weak anchoring can be investigated by means of the "hybrid" cell model described above.

The analysis presented above is valid when $\theta_M(t) \to \pi/2$. Notice, however, that for $t \gg t^*$, $\theta_M(t)$ increases very rapidly and reaches this limiting value even for $t \ll T$ if the condition $T \gg t^*$ is fulfilled. Consequently, the expression for the total current at $t=T$ can be considered as very close to the exact one. This permits to use the measured current to estimate the

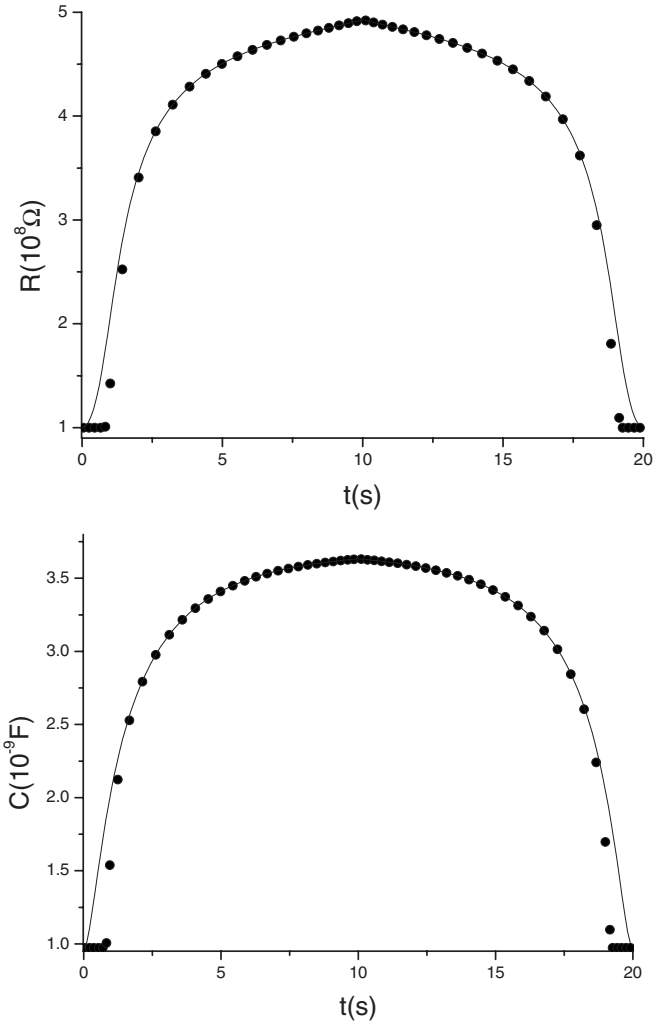

FIG. 9. (a) Comparison of the temporal behavior of the resistance as given by Eq. (15) (solid) with the exact value (dots). (b) The same for the capacitance, as given by Eq. (16) (solid). The curves were drawn for $L/d=0.025$.

extrapolation length of the sample. In fact, one can measure the current near to $t=T$, and by using the closed expression obtained for $R(T)$, $C(T)$, and $I(T)$, together with the nematic parameters, to obtain the ration L/d. In Fig. 11, the behavior of the current at $t=T$ vs the ratio L/d is depicted to illustrate the dependence of the current on the anchoring energy of the sample for some particular set of values of the material parameters. For large values of the ratio L/d, i.e., for negligible anchoring energy, the entire sample tends to a homeotropic behavior and the current reaches a limiting value that corresponds to a horizontal asymptote $[I(T)\approx 23.5$ nA for the parameters we are considering]. Furthermore, the jump in the current near $t=t^*$ and near $t=T$ are not very sensitive to the value of the anchoring energy. This occurs because the discontinuity in the derivative of the capacitance has a negligible dependence on this ratio, as can be seen in Fig. 4. It is also possible to obtain an analytical expression for the current, in which the ratio L/d can be considered as a fitting parameter. First of all, using Eq. (14), it is easy to show that

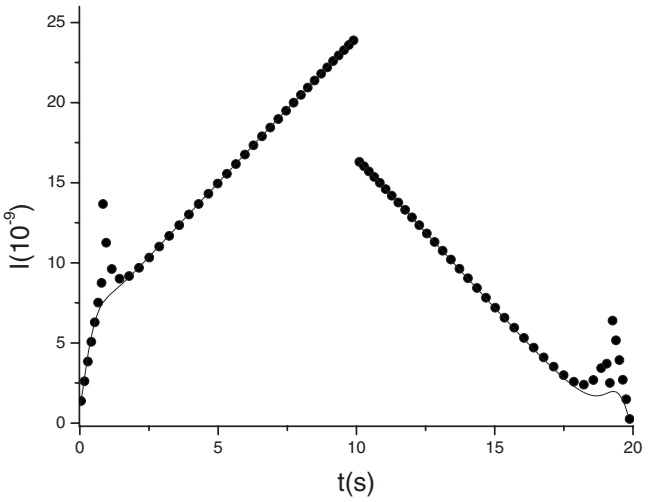

FIG. 10. Comparison of the temporal behavior of the total current obtained in the hybrid cell model (solid) with the exact values (dots) for $L/d=0.025$. Notice that the good agreement between the two curves is not restricted to the interval $t\approx T\approx 10$ s but extends to a large interval.

$$s(t)=\frac{L/\xi(t)-1+\sqrt{1-[L/\xi(t)]^2}}{L/\xi(t)+1-\sqrt{1-[L/\xi(t)]^2}}. \tag{19}$$

On the other hand, we notice that the time dependence of $R(t)$ and $C(t)$ comes exclusively from $\xi(t)$, i.e. $C(t)=C[\xi(t)]$ and $R(t)=R[\xi(t)]$. From the definition of $\xi(t)$ one easily obtains $d\xi(t)/dt=-[\xi(t)/V]dV/dt$. Therefore, according to the above model, the total current is given by

$$I[\xi(t)]=\frac{V(t)}{R[\xi(t)]}+\left\{C[\xi(t)]-\xi(t)\frac{dC(\xi)}{d\xi}\right\}\frac{dV}{dt}, \tag{20}$$

valid for $t^*<t\leq T$ and can be compared with the measured current in order to obtain an estimation for the ratio L/d.

V. CONCLUDING REMARKS

The current-voltage characteristics of a weakly anchored nematic cell submitted to an external voltage changing lin-

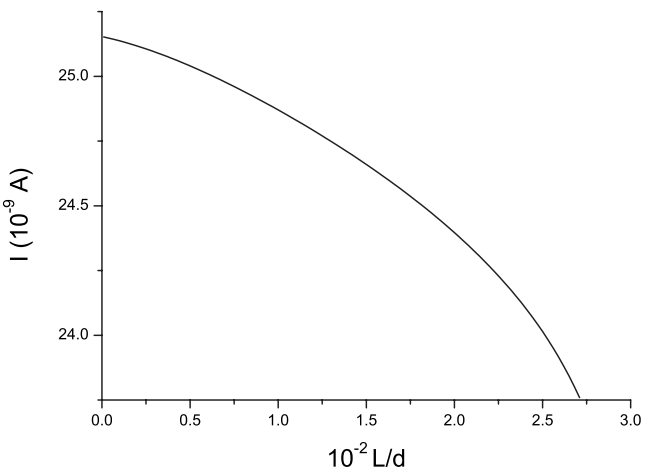

FIG. 11. $I(T)$ as given by Eq. (18) vs L/d.

early with the time, in the quasistatic approximation were analyzed. We have evaluated the contribution to the current related to the reorientation of the nematic molecules when the external voltage overcomes the critical voltage for the transition of Fréedericksz. As in the case of strong anchoring, the current in the external circuit presents a discontinuity at the threshold. We have shown that, at the saturation field, the resistance, R, and the capacitance, C, of the nematic cell reach the values $R_{\parallel}$ and $C_{\parallel}$, corresponding to a homeotropically oriented cell. To get information also on the anchoring strength, the problem was analyzed in the time interval for which $t > t^*$. Since in this interval, $\theta_M(t) \to \pi/2$ rapidly, it is possible to substitute the original cell by a cell formed by two halves in hybrid orientation. In this manner, the profile of the tilt angle is exactly obtained, thus avoiding numerical integrations for the determination of $R(t)$ and $I(t)$. Notice, however, that for $t \gg t^*$, $\theta_M(t)$ increases very rapidly and reaches this limiting value even for $t \ll T$ if the condition $T \gg t^*$ is fulfilled. Consequently, the expression for the total current at $t=T$ obtained in the framework of this approximation can be considered as very close to the exact one. This permits to use the measured current to estimate the extrapolation length of the sample. In principle, one could measure the current near to $t=T$, and by using the closed expression obtained for $R(T)$, $C(T)$, and $I(T)$, together with the nematic parameters, could obtain the ratio L/d and, consequently, the anchoring strength characterizing the surfaces of the sample.

ACKNOWLEDGMENTS

We are grateful to G. Barbero (Italy) for helpful discussion and to the Brazilian Agencies (CNPq and Capes) for financial support.

[1] H. J. Deuling, Mol. Cryst. Liq. Cryst. (Phila. Pa.) **19**, 123 (1972).
[2] P. G. de Gennes and J. Prost, *The Physics of Liquid Crystals* (Oxford University Press, Oxford, 1994).
[3] R. Barberi, F. Ciuchi, G. Lombardo, R. Bartolino, and G. E. Durand, Phys. Rev. Lett. **93**, 137801 (2004).
[4] S. Faetti and P. Marianelli, Phys. Rev. E **72**, 051708 (2005).
[5] L. M. Blinov, E. P. Pozhidaev, F. V. Podgornov, S. A. Pikin, S. P. Palto, A. Sinha, A. Yasuda, S. Hashimoto, and W. Haase, Phys. Rev. E **66**, 021701 (2002).
[6] Shwu-Yun Tsay Tzeng, T. Y. Lin, R. H. Huang, J. J. Wu, and S. L. Wu, Phys. Rev. E **70**, 011712 (2004).
[7] R. Atasiei, A. L. Alexe-Ionescu, J. C. Dias, L. R. Evangelista, and G. Barbero, Chem. Phys. Lett. **461**, 164 (2008).
[8] J. M. S. Pena, I. Perez, V. Urruchi, J. C. Torres, and J. M. Otón, Opto-Electron. Rev. **16**, 189 (2008).
[9] R. Atasiei, A. L. Alexe-Ionescu, C. Dascalu, J. C. Dias, and R. Teixeira de Souza, Phys. Lett. A **372**, 6116 (2008).
[10] T. N. Ruckmongathan, P. Juneja, and A. R. Shashidhara, Proceeding of ASID 2006, 8–12 Oct, New Delhi (unpublished), p. 23.
[11] D. Meyerhofer, in *Introduction to Liquid Crystals*, edited by E. B. Priestley, P. J. Wojtowicz, and Ping Sheng (Plenum Press, New York, 1979).
[12] A. Rapini and M. Papoular, J. Phys. (Paris), Colloq. **30**, C4-54 (1969).
[13] G. Barbero and L. R. Evangelista, *An Elementary Course on the Continuum Theory for Nematic Liquid Crystals* (World Scientific, Singapore, 2001).
[14] G. Barbero, G. Cipparrone, O. G. Martins, and A. M. Figueiredo Neto, Appl. Phys. Lett. **89**, 132901 (2006).
[15] I. W. Stewart, *The Static and Dynamic Continuum Theory of Liquid Crystals* (Taylor & Francis, London, 2004).
[16] P. Kumar, S. N. Patil, U. S. Hiremath, and K. S. Khrishnamurty, J. Phys. Chem. B **111**, 8792 (2007).